

Dynamics of the diluted Ising antiferromagnet $\text{Fe}_{0.31}\text{Zn}_{0.69}\text{F}_2$

K. Jonason^a, P. Nordblad ^a and F. C. Montenegro^b

^aDept. of Materials Science, Uppsala University, Box 534, S-751 21 Uppsala, Sweden

^bDepartamento de Fisica, Universidade Federal de Pernambuco, 50739-901 Recife, PE, Brasil

The diluted Ising antiferromagnet, $\text{Fe}_{0.31}\text{Zn}_{0.69}\text{F}_2$, has been investigated by dynamic susceptibility measurements in zero and finite applied dc-fields. In zero field, there is a para- to antiferromagnetic phase transition at $T_N \approx 20.0\text{K}$, followed by a dramatic slowing down of the dynamics at low temperatures. The latter described by a pure Arrhenius law. The effect of a superposed dc-field on the antiferromagnetic phase transition and on the low-temperature dynamics is investigated, and a comprehensive static and dynamic phase diagram in the $H - T$ plane is derived. In agreement with earlier results on the same system, $T_N(H)$ follows a random-exchange Ising model to random-field Ising model crossover scaling for fields $H \leq 1.5\text{ T}$. A random-field induced glassy dynamics appears for higher values of H , where the antiferromagnetic phase transition is destroyed. The low-temperature dynamics shows striking similarities with the behavior observed in reentrant antiferromagnets.

PACS numbers: 75.40.Gb 75.50.Lk

I. INTRODUCTION

The diluted Ising antiferromagnet $\text{Fe}_x\text{Zn}_{1-x}\text{F}_2$ in an external magnetic field has proven to be a good model system for the random-exchange Ising model (REIM) ($H \approx 0$) and the random field (RFIM) Ising model ($H > 0$)^{1,2}. In the original derivation of the equivalence between the RFIM and a diluted Ising antiferromagnet in a uniform applied field, weak dilution and small values of H/J were assumed³ (J is the magnitude of the exchange interaction). In the $\text{Fe}_x\text{Zn}_{1-x}\text{F}_2$ system, weak dilution implies Fe concentrations well above the percolation threshold⁴ $x_p = 0.25$ and the most convincing experimental results on the RFIM critical behaviour have been obtained on samples with^{1,2} $x \geq 0.46$. On the other hand, interesting dynamic properties may become observable in the limit of strong dilution. RFIM systems have been argued to attain extremely long relaxation times at temperatures near T_c ⁵ and for large values of H/J , where the ordered phase is destroyed, it has been argued that a glassy phase will appear, even without exchange frustration being present in the system⁶. Experimental results on $\text{Fe}_x\text{Zn}_{1-x}\text{F}_2$ samples of concentration at or slightly above x_p have revealed some dynamic properties similar to those of conventional spin glasses⁷⁻¹⁰. In a recent paper¹¹ it was found that the percolating threshold sample $\text{Fe}_{0.25}\text{Zn}_{0.75}\text{F}_2$ exhibits magnetic ageing, a typical spin glass feature, whereas the slowing down of the dynamics followed an Arrhenius law, i.e. it did not support the existence of a finite temperature spin glass phase transition.

Results using neutron scattering¹² and Faraday rotation technique¹³ have established random-field induced spin glass like dynamic behaviour in $\text{Fe}_{0.31}\text{Zn}_{0.69}\text{F}_2$. Recent magnetization experiments revealed that a similar behaviour occur at intense applied fields in samples of $\text{Fe}_x\text{Zn}_{1-x}\text{F}_2$, with $x = 0.56$ and 0.60 ¹⁴. In

this paper we discuss experimental results from dc-magnetisation and ac-susceptibility measurements on the same $\text{Fe}_{0.31}\text{Zn}_{0.69}\text{F}_2$ system of earlier neutron and Faraday rotation measurements. In zero applied field, a slowing down of the dynamics occurs at low temperatures that obeys a pure Arrhenius law and some slowing down is also observable near the antiferromagnetic transition temperature. In applied dc-fields, additional slow dynamical processes are introduced near T_N by the random fields. A comprehensive static and dynamic phase diagram in the $H - T$ plane is deduced that, in parts, adequately compares with an earlier published phase diagram on the same compound¹³.

II. EXPERIMENTAL

A high quality single crystal^{12,13} of $\text{Fe}_{0.31}\text{Zn}_{0.69}\text{F}_2$ in the form of a parallelepiped with its longest axis aligned with the crystalline c -axis was used as a sample. The frequency dependence of the ac-susceptibility in zero applied dc-field was studied in a Cryogenic Ltd. S600X SQUID-magnetometer. A commercial Lake Shore 7225 ac-susceptometer was employed for the ac-susceptibility measurements in a superposed dc magnetic field and the temperature dependence of the magnetisation in different applied dc-fields was measured in a Quantum Design MPMS5 SQUID-magnetometer. The magnetic field was in all experiments applied parallel to the c -axis of the sample.

III. RESULTS AND DISCUSSION

Fig. 1 shows the temperature dependence of both components of the ac-susceptibility, (a) $\chi'(\omega, T)$ and (b)

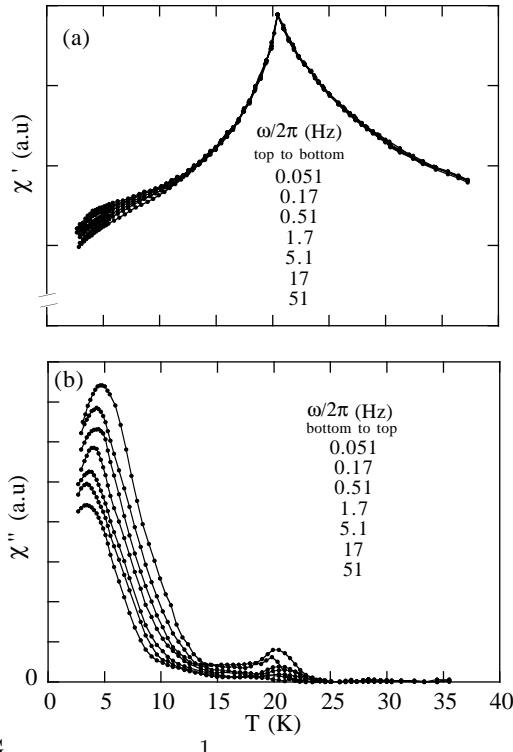


FIG.

1.

Temperature dependence of the ac-susceptibility at different frequencies as indicated in the figures. The probing ac field is 1 Oe. (a) $\chi'(\omega)$ and (b) $\chi''(\omega)$.

$\chi''(\omega, T)$. The different frequencies ranges from 0.051–51 Hz as indicated in the figures. The transition from a paramagnetic Curie-Weiss behaviour at high temperatures to long range antiferromagnetic order is signaled by the cusp in $\chi'(\omega, T)$ at about 20 K. A small bump in $\chi''(\omega, T)$ is observed at about the same temperature. Below 15 K the ac-susceptibility becomes frequency dependent. The out-of-phase component increases and a frequency dependent maximum that shifts towards lower temperatures with decreasing frequency is observed below $T \approx 5$ K. The frequency dependence of $\chi'(\omega, T)$ and $\chi''(\omega, T)$ at low temperatures shows some resemblance with the behaviour of an ordinary spin glass. However, earlier neutron scattering measurements indicated that AF LRO is established below $T_N \approx 19.8$ K in this system¹², provided the sample is submitted to a slow cooling process. To investigate the nature of the slowing down of the dynamics at low temperatures, a comparison is made with the behavior observed in ordinary spin glasses. A 3d spin glass exhibits conventional critical slowing down of the dynamics¹⁵ according to:

$$\frac{\tau}{\tau_0} = \left(\frac{T_f - T_g}{T_g} \right)^{-z\nu}, \quad (1)$$

where τ_0 is the microscopic spin flip time of the order $10^{-13}\text{--}10^{-14}$ s, T_g the spin glass temperature and $z\nu$ a dynamical critical exponent. Defining the inflection point in $\chi''(\omega, T)$ as a measure of the freezing temperature T_f for a relaxation

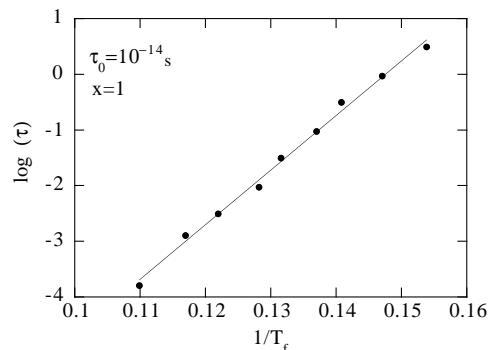


FIG. 2. The best fit of the relaxation times to activated dynamics: $\log \tau$ vs. T_f^{-1} , implying a pure Arrhenius behaviour of the slowing down of the dynamics.

time (τ) corresponding to the observation time, $t \approx 1/\omega$, of the ac-susceptibility measurement, the derived data may be employed for dynamic scaling analyses. The data do not fit conventional critical slowing down according to eq. 1 with physically plausible values of the parameters. Activated dynamics could govern the dynamics still yielding a finite phase transition temperature. The slowing down of the relaxation times should then obey:

$$\ln \left(\frac{\tau}{\tau_0} \right) = \frac{1}{T_f} \left(\frac{T_f - T_g}{T_g} \right)^{-\psi\nu}, \quad (2)$$

where $\psi\nu$ is a critical exponent¹⁶. The derived data fits eq. 2 with $T_g \approx 0$ which implies that the slowing down rather is described by a generalized Arrhenius law:

$$\log \left(\frac{\tau}{\tau_0} \right) \propto T_f^{-x}. \quad (3)$$

Fig. 2 shows the best fit to this expression yielding $x=1$ and $\tau_0=10^{-14}$ s for $0.051 \leq \omega/2\pi(\text{Hz}) \leq 1000$.

The observed frequency dependent ac-susceptibility shows striking similarities with the behaviour of alleged reentrant antiferromagnets. In such a system there is a transition from a paramagnetic phase to an antiferromagnetic phase and spin glass behaviour is observed at low temperatures. The reentrant Ising antiferromagnet $\text{Fe}_{0.35}\text{Mn}_{0.65}\text{TiO}_3$ displays similar features as this system, e.g. the low temperature slowing down of the dynamics is found to obey a pure Arrhenius behaviour¹⁷.

Furthermore, the more diluted system $\text{Fe}_{0.25}\text{Zn}_{0.75}\text{F}_2$ (on the percolation threshold) does not display long range antiferromagnetic order but it exhibits a slowing down of the relaxation times that follows a pure Arrhenius law¹¹ with a similar value of τ_0 as here derived for $\text{Fe}_{0.31}\text{Zn}_{0.69}\text{F}_2$.

In Fig. 3 (a) $\chi'(\omega, T, H)$ and (b) $\chi''(\omega, T, H)$ are plotted for $\omega/2\pi=125$ Hz in different superposed dc magnetic fields $H \leq 2$ T. At these rather low fields, the maximum in $\chi'(\omega, T, H)$ near $T_N(H)$ gets rounded and is pushed towards lower temperature with increasing magnitude of

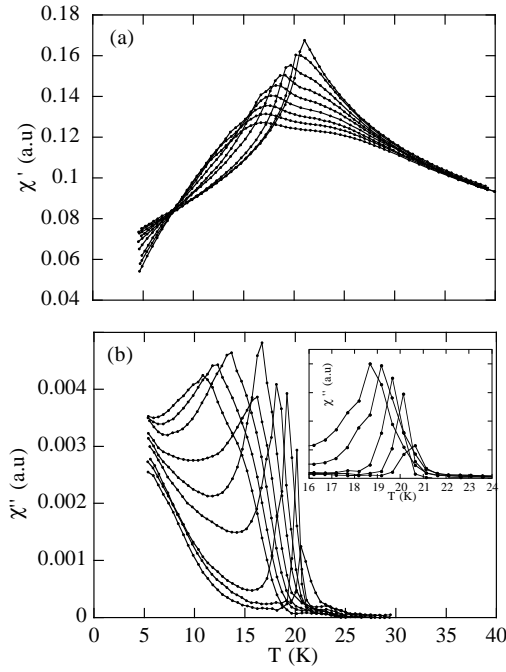


FIG. 3. (a) $\chi'(\omega, T, H)$ and (b) $\chi''(\omega, T, H)$ at $\omega/2\pi=125$ Hz vs. T in different applied dc-fields: 0, 0.25, 0.5, 0.75, 1, 1.25, 1.5, 1.75 and 2 T. The inset in (b) shows $\chi''(\omega, T, H)$ for dc-fields 0.25, 0.375, 0.5, 0.625 T. The amplitude of the ac-field is 10 Oe.

the magnetic field. The corresponding bump in the out-of-phase component in zero dc-field, increases in magnitude and sharpens for increasing dc-fields up to 1 T (the inset of Fig. 3 (b) displays fields up to 0.625 T). A measure of the phase transition temperature $T_N(H)$ is given by the position of the maximum in the derivative $d(\chi' T)/dT^{18}$. For fields $H \leq 1.5$ T, $T_N(H)$ is pushed to lower temperatures with increasing field strength following a REIM to RFIM crossover scaling, as described in ref. 13. At higher fields the maximum is washed out which signals that the antiferromagnetic phase is destroyed. The destruction of the antiferromagnetic phase by strong random fields in $\text{Fe}_x\text{Zn}_{1-x}\text{F}_2$ was observed by earlier Faraday rotation¹³ and neutron scattering¹² measurements in the same system ($x = 0.31$), and by recent magnetization¹⁴ and dynamic susceptibility studies¹⁹ in less diluted samples ($x = 0.42, 0.56$ and 0.60). A glassy dynamics is found in the upper portion of the $H - T$ phase diagram of $\text{Fe}_x\text{Zn}_{1-x}\text{F}_2$, at least within the interval $0.31 \leq x \leq 0.60$.

In increasing applied dc-fields the out-of-phase component is enhanced in a rather narrow but widening region near the antiferromagnetic phase transition due to the introduction of random fields that create new slow dynamical processes in the system. The increase of $\chi''(\omega, T, H)$ at lower temperatures, corresponding to the processes causing the slowing down of the dynamics already in zero field, remains observable also when the field is increased. This latter feature cannot be entirely attributed

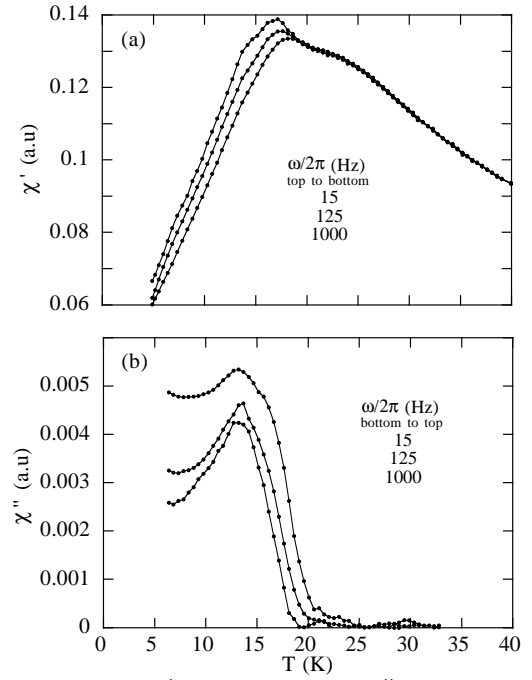


FIG. 4. (a) $\chi'(\omega, T, H)$ and (b) $\chi''(\omega, T, H)$ vs. T in an applied dc-field $H=1.5$ T and at different frequencies $\omega/2\pi=15, 125$ and 1000 Hz. The amplitude of the ac-field is 10 Oe.

to random fields. For larger fields these low temperature processes and the processes caused by the random fields start to overlap, and at the highest dc-fields they even become indistinguishable. In Fig. 4 both components of the ac susceptibility are plotted, in an applied dc-field $H=1.5$ T, for $\omega/2\pi=15, 125$ and 1000 Hz. Note that the temperature of the maximum in $\chi'(\omega, T, H)$, at $T_N(H)$, shifts to lower temperatures as the frequency decreases. By way of contrast, no shift in the peak temperature is observable as a function of the frequency in dynamic susceptibility measurements performed in $\text{Fe}_{0.46}\text{Zn}_{0.54}\text{F}_2^{20}$ and $\text{Fe}_{0.42}\text{Zn}_{0.58}\text{F}_2^{19}$, within the field limits of the weak RFIM problem in each case. The frequency dependent behaviour of $T_N(H)$ is a feature associated with the effects of strong random fields in samples of $\text{Fe}_x\text{Zn}_{1-x}\text{F}_2$, particularly with x close to x_p .

In Fig. 5 (a) and (b) $\chi'(\omega, T, H)$ and $\chi''(\omega, T, H)$ are plotted for $\omega/2\pi=125$ Hz in different superposed dc magnetic fields $H \geq 2$ T. The maximum in the in-phase-component is flattend, the susceptibility is strongly suppressed and the onset of the out-of-phase susceptibility is shifted towards lower temperatures as the dc-field is increased. No sign of a transition to an antiferromagnetic phase is observed.

Fig. 6 shows the temperature dependence of the field cooled (FC), $M_{FC}(T)/H$, and zero field cooled (ZFC), $M_{ZFC}(T)/H$, susceptibility²¹ at three different applied magnetic fields. Below a temperature T_{ir} the magnetisation becomes irreversible. T_{ir} decreases with increasing

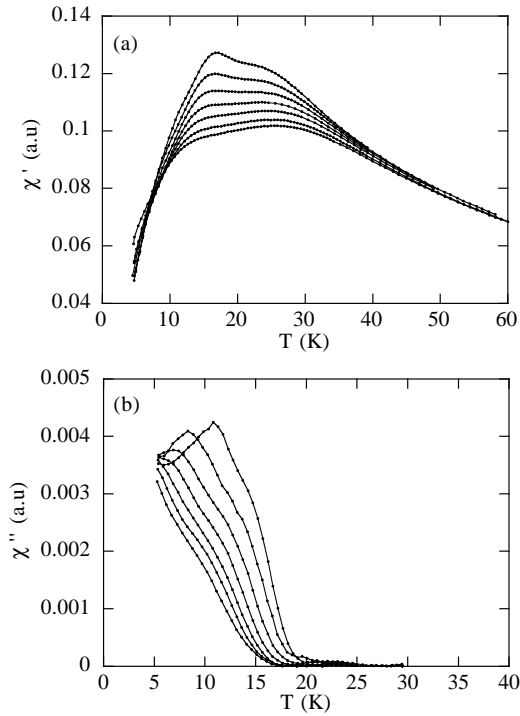


FIG. 5. (a) $\chi'(\omega, T, H)$ and (b) $\chi''(\omega, T, H)$ at $\omega/2\pi=125$ Hz vs. T in different applied dc-fields: 2, 2.5, 3, 3.5, 4, 4.5 and 5 T. The amplitude of the ac-field is 10 Oe.

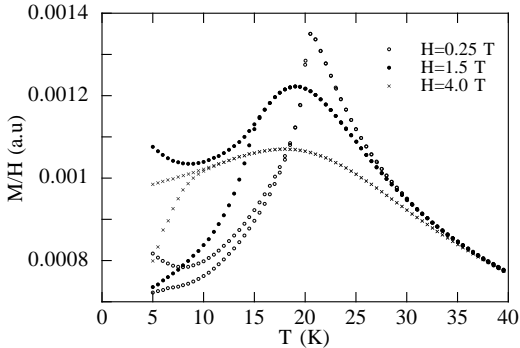


FIG. 6. Temperature dependence of the dc-susceptibility for zero-field-cooled (ZFC) and field-cooled (FC) procedures in different fields, as indicated in the figure.

field. The irreversibility point is associated with an observation time mainly governed by the heating rate of the ZFC experiment which in our experiment corresponds to about 100 s.

In Fig. 7 an $H - T$ magnetic phase diagram is shown, in which some of the above discussed experimental characteristics are summarised. The open circles represent $T_N(H)$, the solid circles $T_{ir}(H)$, diamonds the spin freezing temperatures $T_f(H)$ for $\omega/2\pi=125$ Hz and open triangles label $T_f(H=0)$ for different frequencies. The onset of $\chi''(\omega, T, H)$ at frequencies $\omega/2\pi=15, 125$ and 1000 Hz are shown as solid triangles, solid squares and open squares respectively. Those are measures that mirror the observation time dependence of T_{ir} .

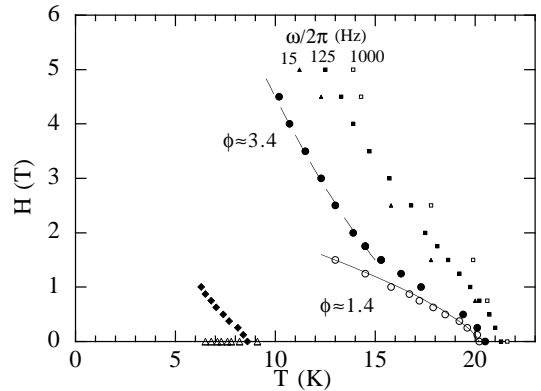


FIG. 7. $H - T$ diagram of the $\text{Fe}_{0.31}\text{Zn}_{0.69}\text{F}_2$ system. $T_N(H)$ open circles, $T_{ir}(H)$ solid circles, onset of $\chi''(\omega, T, H)$ for $\omega/2\pi=15$ (solid triangles), 125 (solid squares) and 1000 Hz (open squares), $T_f(H, \omega/2\pi=125$ Hz) diamonds and $T_f(H=0)$ triangles for different frequencies $\omega/2\pi$ (from left to right): 0.051, 0.17, 0.51, 1.7, 5.1, 17, 51, 125 and 1000 Hz.

In diluted Ising antiferromagnets, T_N is expected to decrease with increasing magnetic fields as:

$$\epsilon \propto H^{2/\phi} \quad ; \quad \epsilon = \left(\frac{T_N(H) - T_N(0) + bH^2}{T_N(0)} \right) \quad (4)$$

where ϕ is a crossover exponent and bH^2 a small mean field correction. For low fields, $H \leq 1.5$ T, we find $\phi \approx 1.4$ using $b=0$ for $T_N(H)$ as indicated by the solid line in Fig. 7. For higher fields, $H \geq 1.5$ T, a reversal of the curvature of $T_{ir}(H)$ occurs. The dashed line corresponds to a functional behaviour according to eq. 4 with an exponent $\phi \approx 3.4$. A largely equivalent phase diagram has earlier been established for the same system utilising Faraday rotation measurements¹³. One significant difference being that $T_{ir}(0) \approx T_N(0)$ in ref.¹³, whereas we find a significant difference between these two temperatures, as is also observed in other dilute antiferromagnets²². The field dependence of $T_N(H)$ is equivalent to those of the more concentrated $\text{Fe}_{0.46}\text{Zn}_{0.54}\text{F}_2$ and $\text{Fe}_{0.72}\text{Zn}_{0.28}\text{F}_2$ where the scaling behaviour of eq. 4 gives $\phi \approx 1.4$ for fields up to 2 T and 10 T respectively²³. The new features of the phase diagram in Fig. 7 as compared to the one of ref.¹³ are the observation time dependent spin freezing temperatures at low temperature and the observation time dependence of $T_{ir}(H)$ demonstrated by the shifts of the $T_{ir}(H)$ contours towards higher temperatures when decreasing the observation time. A possible mechanism for the spin freezing at low temperatures may be a weak frustration present in a third nearest neighbour interaction of this compound. Results of numerical simulation²⁴ indicates that a small frustrated bond plays no role in the REIM properties of $\text{Fe}_x\text{Zn}_{1-x}\text{F}_2$ under weak dilution. However, it causes dramatic influences in the antiferromagnetic and spin glass order parameters close to the percolation threshold.

IV. CONCLUSIONS

Dynamic and static magnetic properties of the diluted antiferromagnet $\text{Fe}_{0.31}\text{Zn}_{0.69}\text{F}_2$ have been studied. The dynamic susceptibility in zero dc-field shows similarities to a reentrant Ising antiferromagnet with a slowing down of the dynamics at low temperatures best described by a pure Arrhenius law. Hence, there is no transition to a spin glass phase at low temperatures.

The field dependence of the antiferromagnetic transition temperature follows the predicted scaling behaviour for a random field system, in accord with earlier experimental findings^{13,23}. The onset of $\chi''(\omega, T, H)$ occur above the antiferromagnetic phase transition, even in zero applied magnetic field. $\chi''(\omega, T, H)$ shows a frequency dependent behaviour that mirror the observation time dependence of the FC-ZFC irreversibility line. The dynamics of the diluted antiferromagnet $\text{Fe}_{0.31}\text{Zn}_{0.69}\text{F}_2$ has been shown to involve not only random field induced slow dynamics near $T_N(H)$, but additional slow dynamics originating from the strong dilution appears at low temperatures.

V. ACKNOWLEDGMENTS

Financial support from the Swedish Natural Science Research Council (NFR) is acknowledged. One of the authors (FCM) acknowledge the support from CNPq and FINEP (Brazilian agencies).

- ⁵ A. J. Bray, *J. Phys. C* **16**, 5875 (1983).
- ⁶ J. R. L. de Almeida and R. Bruinsma, *Phys. Rev. B* **37**, 7267 (1987).
- ⁷ F. C. Montenegro, S. M. Rezende and M. D. Coutinho-Filho, *J. Appl. Phys.* **63**, 3755 (1988); *ibid. Europhys. Lett.* **8**, 383 (1989).
- ⁸ S. M. Rezende, F. C. Montenegro, M. D. Coutinho-Filho, C. C. Becerra and A. Paduan-Filho, *J. Phys. (Paris) Colloq.* **49**, c8-1267 (1988).
- ⁹ F. C. Montenegro, U. A. Leitao, M. D. Coutinho-Filho and S. M. Rezende, *J. Appl. Phys.* **67**, 5243 (1990).
- ¹⁰ S. M. Rezende, F. C. Montenegro, U. A. Leitao and M. D. Coutinho-Filho, in *New Trends in Magnetism* edited by M. D. Coutinho-Filho and S. M. Rezende (World Scientific, Singapore, 1989), p. 44.
- ¹¹ K. Jonason, C. Djurberg, P. Nordblad and D. P. Belanger, *Phys. Rev. B* **56**, 5404 (1997).
- ¹² D. P. Belanger, Wm. E. Murray Jr, F. C. Montenegro, A. R. King, V. Jaccarino and R. W. Erwin, *Phys. Rev. B* **44**, 2161 (1991).
- ¹³ F. C. Montenegro, A. R. King, V. Jaccarino, S-J. Han and D. P. Belanger, *Phys. Rev. B* **44**, 2155 (1991).
- ¹⁴ F. C. Montenegro, K. A. Lima, M. S. Torikachvili, A. H. Lacerda, *J. Magn. Magn. Mater.* **177-181**, 145 (1998); *ibid. in Magnetism Magnetic Materials and their Applications* edited by F. P. Missel (Trans Tech Publications Ltd, Switzerland, 1999), p. 371.
- ¹⁵ P. C. Hohenberg and B. I. Halperin, *Rev. Mod. Phys.* **49**, 435 (1977).
- ¹⁶ D. S. Fisher and D. A. Huse, *Phys. Rev. B* **38**, 373 (1988); **38**, 386 (1988).
- ¹⁷ K. Jonason, P. Nordblad and A. Ito, unpublished.
- ¹⁸ M.E. Fisher, *Phil. Mag.* **7**, 1731 (1962).
- ¹⁹ A. Rosales-Rivera, J. M. Ferreira and F. C. Montenegro, unpublished.
- ²⁰ A. R. King, J. A. Mydosh and V. Jaccarino, *Phys. Rev. Lett.* **56**, 2525 (1986).
- ²¹ Susceptibility is here defined and calculated as M/H .
- ²² P. Nordblad, J. Mattsson, W. Kleemann, *J. Magn. Magn. Mater.* **140-144**, 1553 (1995).
- ²³ A. R. King, V. Jaccarino, D. P. Belanger and S. M. Rezende, *Phys. Rev. B* **32**, 503 (1985).
- ²⁴ E. P. Raposo, M. D. Coutinho-Filho and F. C. Montenegro, *Europhys. lett.* **29** 507 (1995); *ibid. J. Magn. Magn. Mater.* **154**, L155 (1996).